



Islamic Azad University



## First-Principles Study of Structure, Electronic and Optical Properties of HgSe in Zinc Blende (B3) Phase

Hamdollah Salehi<sup>\*1</sup>, Firoozeh Anis Hoseini<sup>1</sup>

<sup>1</sup> Department of Physics, Faculty of Science, Shahid Chamran University, of Ahvaz, Ahvaz, Iran

(Received 10 Apr. 2019; Revised 11 May 2019; Accepted 20 May 2019; Published 15 Jun. 2019)

**Abstract:** In this paper, the structural parameters, energy bands structure, density of states and charge density of HgSe in the Zinc blende (B3) phase have been investigated. The calculations have been performed using the Pseudopotential method in the framework of density functional theory (DFT) by Quantum Espresso package. The results for the electronic density of states (DOS) show that the band gap for HgSe is zero. The obtained energy bands structure for HgSe show that the lowest conduction band minimum and the top of the valence band are degenerate at the center of Brillouin zone ( $\Gamma$ ), and this compound is a zero-gap material or semimetal. Calculation of electron charge density in zinc blende phase in (110) plane show that this compound has ionic and covalent bond simultaneously. The theoretical calculated optical properties and energy Loss (EEL) spectrum yield a static refractive index of 4.37 and a plasmon energy of 22.83 eV for cubic phase. This calculation are in good agreement with the other theoretical and experimental values.

**Keywords:** Energy Bands Structure, Mercury Selenide, Pseudopotential, Quantum Espresso. Density Functional Theory

### 1. INTRODUCTION

Timannite is a mineral, mercury selenide, formula HgSe. It occurs in hydrothermal veins associated with other selenides, or other mercury minerals such as cinnabar, and often with calcite. HgSe discovered in 1855 in Germany, it is named after C. W. Tiemann (1848-1899) [1]. Mercury Selenide belongs to II-VI family of semiconductors crystallizing in the zinc blende structure [2]. Based on its electrical properties, it is classified as a semimetal or degenerate semiconductor [3]. Due to high mobility of the electrons this material is an ideal matrix to study additional quantization effects in low-dimensional structures and semimagnetic properties [2]. The cubic Hg II-VI systems  $\beta$ -HgS, HgSe, and HgTe are technologically interesting materials with application in quantum electronics [4] and thermoelectric coolers [5]. They form part of several artificial

\* Corresponding author. Email: [salehi\\_h@scu.ac.ir](mailto:salehi_h@scu.ac.ir)

nanostructured materials [4]. To get low-resistance ohmic contacts has been a major problem in the technology of optical devices based on ZnSe. But the recent studies have proved the possibility of the ohmic contact between HgSe and ZnSe comparable to the case of HgTe on CdTe. There has also been a great interest towards ternary alloy thin films containing HgSe as a host material in spintronic and optoelectronic devices such as IR detectors, IR emitters and tunable lasers[6].The zinc blende structure of HgSe with space group  $F\bar{4}3m(216)$  shown in Fig1.

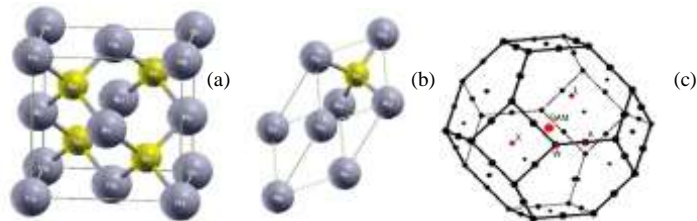


**Fig.1.** (a) Conventional unit cell, (b) primitive unit cell and (c) first brillouin zone for B3 structure of HgSe

HgSe and HgTe appear to have similar behavior under compression. Their ambient-pressure (semimetallic) zinc-blende phases transform first into a semiconducting cinnabar-type structure at the very low “high pressure” of  $\sim 1$  GPa which on further compression transforms into a NaCl phase. A second, very close transition from zb to an orthorhombic phase with space group  $C2221$ , which is a distortion of Zb, has been reported at pressures slightly above the onset of the zb  $\rightarrow$  cinn transition, in the region of coexistence of the zb and cinn phases. This “hidden”  $C2221$  transition is therefore formed when the zb phase is already thermodynamically unstable with respect to the cinn phase, though it has not yet completely transformed to cinn as a result of the sluggish kinetics of the transition. The  $C2221$  phase further transforms into the cinn phase upon slight pressure increase. There is a further transition at 25–30 GPa in HgSe to a phase which has been identified as site-ordered  $Cmcm$ , and which, as in most other cases of reported  $Cmcm$  phases, had been previously characterized as b-Sn-type or bct-type. This is a first-order transition, although the change in volume is very small. There are no further transitions up to the highest pressures reached of about 50 GPa[7-9].

## 2. METHOD OF CALCULATION

The calculations have been performed using plane wave with Pseudopotential method in the framework of the DFT with the local density approximation (LDA) using PWscf package[10,11]. The valance orbitals that the calculations performed only for them for Hg and Se atoms are 5d,6s,6p and 4s,4p respectively. The used experimental lattice constant in calculation is  $6.085\text{\AA}$

[12]. The cutoff energy, which defines the separation between the core and the valence states, was set to 28 Ry. We used  $12 \times 12 \times 12$  Monkhorst Pack meshes which generated 72 k-points in the first Brillouin zone. The self-consistent cycles is converged in five cycles and the total energy converged to better than  $8 \times 10^{-8}$  Ry.

### 3. RESULTS AND DISCUSSION

#### 3.1. Structural properties

One of the important parameters in these calculations is the lattice constant. This constant have been measured experimentally, however, theoretical issue must be calculated for confirming. We are calculated the total energy as a function of volume within LDA approach for HgSe in B3 phase .Fig. 2 indicates the total energy versus volume in LDA approximation. In this calculations, we are used the experimental lattice constant as the starting point and fitted the results with a Mornagan equation of states (EOS). The calculated equilibrium lattice constant  $a(\text{\AA})$ , equilibrium volume  $V(\text{\AA}^3)$ , bulk modulus  $B(\text{GPa})$ , the pressure derivative of the bulk modulus( $B'$ ), Compressibility  $K(\text{kbar})$  and equilibrium total energy  $E(\text{Ry})$  for B3 phase, are summarized in Table 1 that contains results of the previous theoretical calculations in addition to the experimental data for comparison. The present results agree well with the previous experimental and theoretical reports.

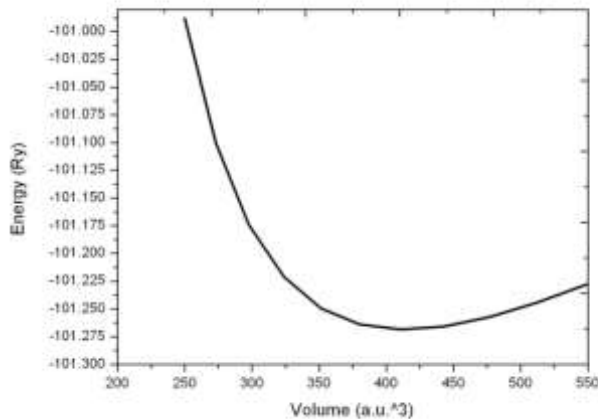


**Fig.2.** Calculated total energies as a function of volume for HgSe in LDA approach

**Table1.** The calculation structure parameters in this work and compared with other results for cubic HgSe

Quantity	Present work		Other work	
	LDA	GGA	Experimental results	Theoretical results
a(Å)	6.089	6.256	6.085[12,13]	6.464[4]
Percent error with the experimental results	0.06	2.81	-	6.23
V(Å) <sup>3</sup>	56.444	61.224	56.2[15]	61.4[4]
Percent error with the experimental results	0.43	8.94	-	9.25
B (kbar)	531	442	500[8,9,12,13]	588[4]
Percent error with the experimental results	6.2	11.6	-	17.6
B'	4.81	4.67	-	-
K (kbar) <sup>-1</sup>	1.88×10 <sup>-3</sup>	2.26×10 <sup>-3</sup>	-	-
E(Ry)	-101.564	-101.268	-	-

### 3.2. Band structure and density of state

In a simple chemical picture of the Hg II–VI semiconductors, Hg contributes with two *s* electrons to the bonding and the chalcogen with two *s* and four *p* electrons. In the Hg II–VI compounds, the bondings are rather covalent and dominated by *sp*<sup>3</sup> hybrids, as indicated by the tetrahedral coordination [14]. In comparison with the Ca, Sr, and Ba chalcogenides the ionicity of the Hg chalcogenides is reduced. The Hg *d* electrons are partially delocalized, and therefore the effective nuclear charge experienced by the valence electrons is increased. This causes that Hg valence *s* electrons be bounded more tightly. Hence, it has a less ionic and more covalent bond. In this respect, these systems are very similar to the electronic Cd and Zn II–VI semiconductors. The *d*-shell delocalization is stronger in Hg than in Cd or Zn and in fact so strong that it causes the *s* level to be pulled down below the chalcogen *p* level; i.e., an inverted band structure is formed [4]. If we consider the usual definition of the band gap, which is the difference between the top of the valence band  $\Gamma_8$  and the lowest conduction band  $\Gamma_6$ , then these gaps come out to be negative. The Hg *s* level, a conduction-band minimum (CBM) forming a state of  $\Gamma_6$  symmetry, is pulled down below the *p*-like  $\Gamma_8$  level which is the valence-band maximum (VBM). It happens due to the large effective positive charge of the Hg core. Because the CBM is found below the VBM, these materials lead to an interesting class of materials so-called ‘inverted band-structure materials’ (Fig. 3) [15]. In Fig. 3 the energy bands for HgSe at the  $\Gamma$  point are shown, there are no gap at the Fermi energy level and the gap between  $\Gamma_6$  level and  $\Gamma_8$  level is negative.

Investigation of the energy bands structure is suitable way for identification of many properties of the materials. The calculated electronic band structure of the cubic phase of HgSe in the high symmetry directions in the Brillouin zone is shown in Figure 4. As it can be seen, the calculated energy bands have been

distributed in the energy range -14 to +14 eV. The Fermi level is set in zero energy. The band gap is zero at  $\Gamma$  point in the Brillouin zone, in the Fermi level within our approach. So HgSe is a semimetal and this result agree well with the previous experimental and theoretical results in references [4,15].

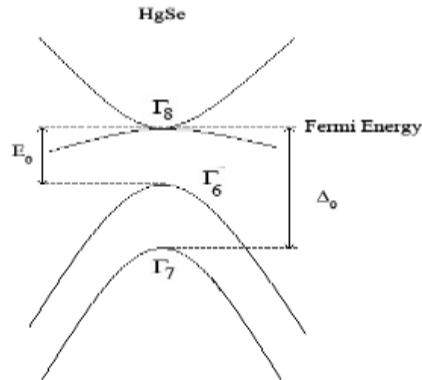


**Fig.3.**The inverted band structure for HgSe; this is a zero band gap in Fermi energy[16].

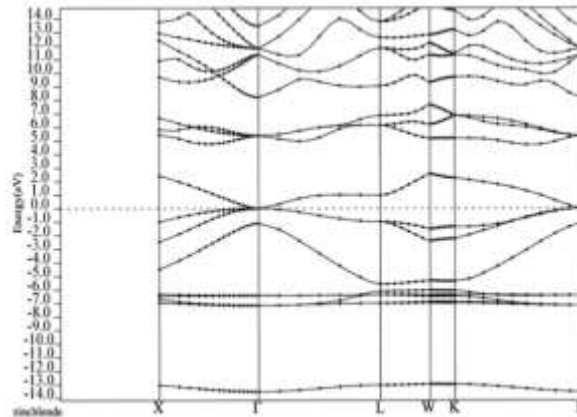


**Fig.4.**The calculated band structure for HgSe in zinc blende phase.

The electron distribution in an energy spectrum is described by the density of states (DOS). It can be measured in photoemission experiments. We have calculated the partial and total density of states using LDA approximation for B3 phase of HgSe. The partial and total density of states are presented in Fig 5. The calculated total density of states suggested that the lower part of the valence band is dominated by the Se-4s orbital and the other part is influenced by the Hg-5d orbital in HgSe. The lower part of the conduction band is dominated by the Hg-6p and Se-4p orbitals, so there is hybridization between mercury 6p states and selenium 4p states, that causes the strong covalent interaction of the Hg-Se bonds in HgSe. From Fig. 5, we found that HgSe in B3 phase is a semimetal or a semiconductor with a direct gap of 0 eV at the Fermi energy in

agreement with theoretical value in [4,15], but this band gap is smaller than the experimental value (0.42 eV) in [17].

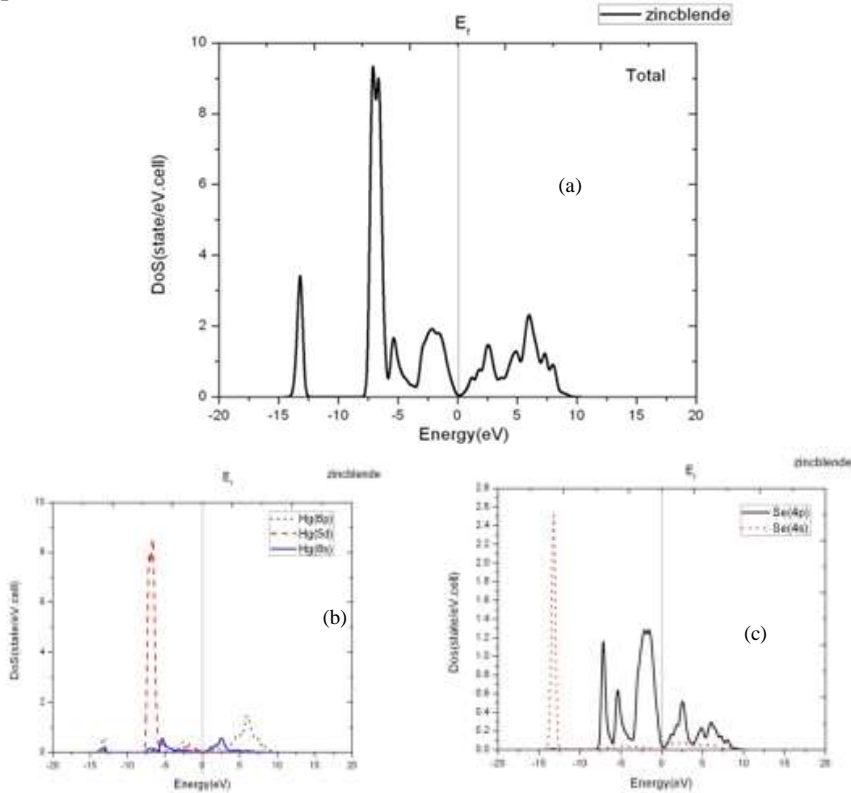


**Fig.5.** (a)The total DOS and the partial DOS for the (b) Hg and (c) Se orbitals are computed in the LDA scheme.

### 3.3. Charge density distribution

The bonding properties of the solids can be described accurately using total contour plots of valence charge density distribution. The contour plots of total valence charge density distribution for HgSe in the (110) plane in two dimensions have been shown in Fig6. In B3 structures there are strong covalent interactions of the Hg-Se bonds in HgSe. Hence HgSe has ionic and covalent bond simultaneously.

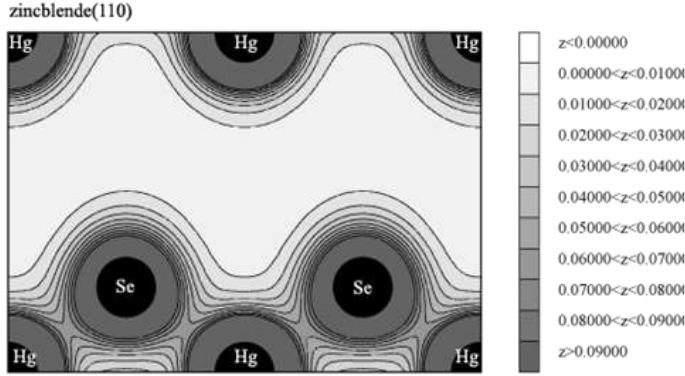


**Fig.6.**Contour plot of the electron density in the (110) plane for B3 phase of HgSe.

#### 4.OPTICAL PROPERTIES

Optical properties of the material can be described with complex dielectric function  $\varepsilon(\omega)$ . As it is obtained other optical parameters also can be set properly. Since the HgSe compound has cubic symmetry, it is needed to calculate only one dielectric tensor component to fully characterize the linear optical properties. Dielectric function,  $\varepsilon(\omega)$ , is the frequency dependent.  $\varepsilon_2(\omega)$ , the imaginary part of the frequency dependent dielectric function, is given by[8,18]:

$$\varepsilon_2(\omega) = \frac{\hbar e^2}{\pi m^2 \omega^2} \sum_{c,v} \int_{BZ} |M_{cv}(k)|^2 \delta[\omega_{cv}(k) - \omega] dk^3 \quad (1)$$

The integral is over the first Brillouin zone. The momentum dipole elements,  $M_{cv}(k) = \langle u_{ck} | \delta \cdot \nabla | u_{vk} \rangle$ , are matrix elements for direct transitions between valence  $u_{vk}$  and conduction band  $u_{ck}$  states, where  $\delta$  is the potential vector describing the electric field, and the energy  $\hbar\omega_{cv}(k) = E_{ck} - E_{vk}$  is the corresponding transition energy. The real part  $\varepsilon_1(\omega)$  of the frequency dependent dielectric function can be obtained from the imaginary part using the Kramers–Kronig relation[19].

$$\varepsilon_1(\omega) = 1 + \frac{2}{\pi} P \int_0^{\infty} \frac{\omega' \varepsilon_2(\omega')}{\omega'^2 - \omega^2} d\omega' \quad (2)$$

where,  $P$ , refer to the principal value of the integral. The information about both real and imaginary parts of the dielectric function allows the calculation of important optical functions such as the refractive index  $n(\omega)$  and extinction coefficient:

$$n(\omega) = \left[ \frac{\varepsilon_1(\omega)}{2} + \frac{\sqrt{\varepsilon_1^2(\omega) + \varepsilon_2^2(\omega)}}{2} \right]^{1/2} \quad (3)$$

$$k(\omega) = \left[ \frac{\sqrt{\varepsilon_1^2(\omega) + \varepsilon_2^2(\omega)}}{2} - \frac{\varepsilon_1(\omega)}{2} \right]^{1/2} \quad (4)$$

At the low frequency ( $\omega \approx 0$ ), the following relation can be derived:

$$n(0) = \sqrt{\varepsilon(\omega)}, \quad (5)$$

In the calculations of the optical properties, a dense mesh of the uniformly distributed k-points is required. Hence, the Brillouin zone integration was performed with 216 points in the irreducible part of the Brillouin zone. We calculated both the electronic and optical properties of HgSe in the cubic phase, but here we only present the optical properties. The real and the imaginary parts of the dielectric functions are shown in Figure7 for HgSe in the cubic phase. The value of the main peak of  $\varepsilon_1(\omega)$  curve is -10 at the energy of 2.5eV and for  $\varepsilon_2(\omega)$  is 3 at the energy equal 4eV.

The static refractive index value for HgSe in the cubic phase calculated in this work and the values obtained by other methods are summarized in Table2. Referring to Table2, it can be seen that the calculated refractive index in this work is smaller than the values measured experimentally. This difference may be mainly due to the calculated Pseudopotential method .

**Table2.** The Calculation static refractive index in this work and compared with other results for cubic HgSe.

Quantity	Present work		Other work	
	LSDA	GG A	Experimental results[8, 20]	Theoretical results[21]
$\varepsilon(\omega)$	17.35	19.1	25.6	14.2
Percent error with the experimental results	32.2	25.4	-	44.53
(n) Refractive index	4.17	4.37	5.06	3.77
Percent error with the experimental results	17.59	13.6 4	-	25.49

As seen in the Figure7a the real part of dielectric function in the zero energy,  $\varepsilon(0)$ , of the Zinc blende phase of HgSe is negative, then a maximum energy intensity is the amount dropped 1eV and finally around the zero point can be converted to a straight line. Due to the nature of the interest metallic HgSe, regardless of the actual contribution of spin interactions real part of

dielectric, the negative phase is obtained, the refractive index cannot be calculated. Due to the imaginary part Figure (7b), the maximum absorption energy 1.8 eV takes place.

The optical band gap  $E_g$  is another important quantity that characterizes semiconductors and dielectric materials because it has a considerable significance in the design and modeling of such materials. Optical band gap obtained from the imaginary part of the dielectric function near the band gap obtained from the band structure has a good agreement.

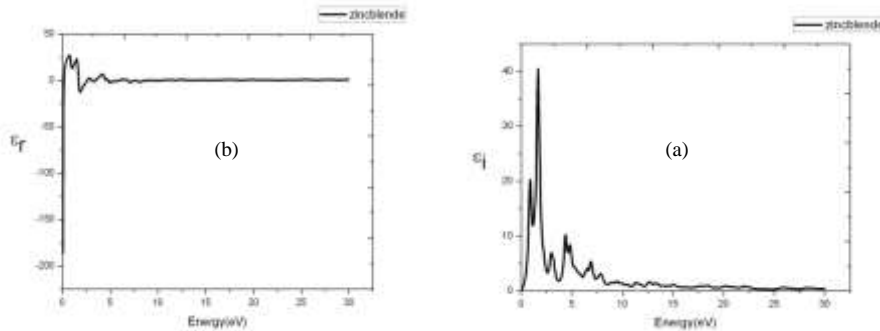


**Fig.7.** Calculated real and imaginary parts of the dielectric function of HgSe with LDA approximation

**4.1 Electron Energy Loss Spectroscopy:** EELS is a valuable tool for investigating various aspects of materials[12]. It has the advantage of covering the complete energy range including non-scattered and elastically scattered electrons (Zero Loss). At intermediate energies (typically 1 to 50 eV) the energy losses are due primarily to a complicated mixture of single electron excitations and collective excitations (plasmons). The positions of the single electron excitation peaks are related to the joint density of states between the conduction and valence bands, whereas the energy required for the excitation of bulk plasmons depends mainly on the electron density in the solid. Here electrons, which excite the atoms electrons of the outer shell is called Valence Loss or valence interband transitions. At higher energies, typically a few hundred eV, edges can be seen in the spectrum, indicating the onset of excitations from the various inner atomic shells to the conduction band. In this case the fast electrons excite the inner shell electrons (Core Loss) or induce core level excitation of Near Edge Structure (ELNES) and XANES. The edges are characteristic of particular elements and their energy and height can be used for elemental analysis.

In the case of interband transitions, which consist mostly of plasmon excitations, the scattering probability for volume losses is directly connected to the energy loss function. One can then calculate the EEL spectrum from the following relations.

$$\varepsilon_{\alpha\beta}(\omega) = \varepsilon_1 + i\varepsilon_2 \quad \text{and} \quad \text{EELSpectrum} = \text{Im}[-1/\varepsilon_{\alpha\beta}(\omega)] = \frac{\varepsilon_2}{\varepsilon_1^2 + \varepsilon_2^2} \quad (6)$$

In Figure (8) the energy loss function is plotted for HgSe in cubic phase. These peaks can, however, have different origins such as charge carrier plasmons and interband or intraband excitations. The energy of the maximum peak of  $\text{Im}[-\varepsilon^{-1}(\omega)]$  at 22.83eV is assigned to the energy of the volume plasmon  $\hbar\omega_p$ . The value of  $\hbar\omega_p$  obtained in this work and for free electron is given in Table 3. For free electrons the plasmon energy is calculated according to the following model:

$$\hbar\omega_p^e = \hbar \sqrt{\frac{ne^2}{\varepsilon_0 m}} \quad (7)$$

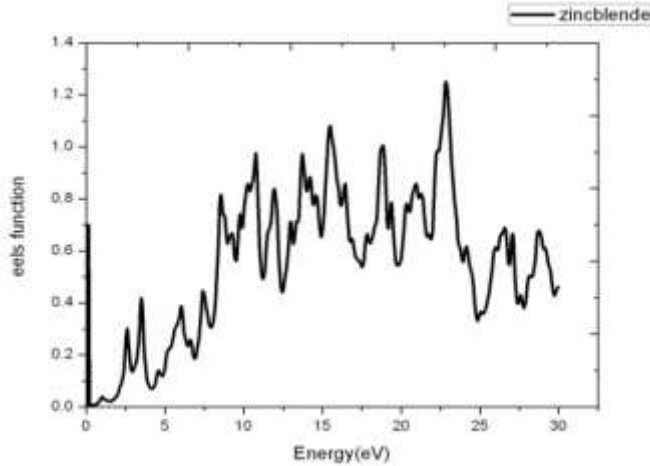


**Fig. 8.** Electron energy loss spectrum  $\text{Im}[-\varepsilon^{-1}(\omega)]$  for HgSe in cubic phase.

**Table3.** The plasmon energy  $\hbar\omega_p$  of the energy loss function in cubic phase calculated by this method and free electron.

Quantity	Present work	Other work
Plasmon energy $\hbar\omega_p$ (eV)(this work)	16.92	-
Plasmon energy $\hbar\omega_p$ (eV)( Free electron)	20.98	-

## 5. CONCLUSION

The structural and electronic properties of HgSe in B3 phase have been investigated using the pseudopotential method. The structure parameters are calculated using LDA approximation are in better agreement with the

experimental values. From the band structures, we found that HgSe is a semiconductor with a direct gap of 0eV or semimetal in B3 phase that the total and partial density of states confirm it. Density of states analysis showed that there is hybridization between mercury 6p states and selenium 4p states, it causes the strong covalent interaction of the Hg-Se bonds in HgSe. The calculated electron density denotes that HgSe has ionic and covalent bond simultaneously. In this paper, we found that the results obtained for B3 phase of HgSe, from the LDA method, are generally in better agreement with the experimental value than other theoretical calculations. The optical parameters such as  $\epsilon(\omega)$  and  $n(\omega)$  were also be calculated and analyzed and it was found static refractive index about 4.37. Considering the spin polarization of the optical properties of the Zinc blende phase calculations, the results for the the real and imaginary dielectric and the plasmons energy changes that Caused by nature semi metallic phase is interesting.

## REFERENCES

- [1] L. Jiajun, Z. Minghua, L. Wenquan, *Tiemannite from a micro-disseminated gold deposit in Qiongmo*, J. Chengdu Institute of Technology. 23 (2), (1996) 21-28.  
[http://en.cnki.com.cn/Article\\_en/CJFDTOTAL-CDLG602.003.htm](http://en.cnki.com.cn/Article_en/CJFDTOTAL-CDLG602.003.htm)
- [2] J. Stolpe, O. Portugal, N. Puhmann, H. -U. Mueller, *Intra and inter-band transitions in HgSe in magagauss fields*, J. Phys. B 294, (2001) 459-462.  
<https://www.sciencedirect.com/science/article/pii/S0921452600006992>
- [3] V. Venkatasamy, M. K. Mathe, S. M. Cox, U. Happek, J. L. Stickney, *Optimization Studies of HgSe thin film deposition by electrochemical atomic layer epitaxy*, J. Electrochemical Acta. 51, (2006) 4347-4351.  
<https://www.sciencedirect.com/science/article/pii/S0013468605013927>
- [4] A. Delin, T. Kluner, *Excitation Spectra and ground-state properties from density-functional theory for the inverted bandstructure systems  $\beta$ -HgS, HgSe and HgTe*, Phys. Rev. B 66, (2002) 1-8.  
<https://journals.aps.org/prb/abstract/10.1103/PhysRevB.66.035117>
- [5] M. K. Mathe, S. M. Cox, V. Venkatasamy, U. Happek, J. L. Stickney, *Formation of HgSe thin films using Electrochemical Atomic Layer Epitaxy*, J. Electrochemical Society. 152(11), (2005) 751-755.  
<http://jes.ecsdl.org/content/152/11/C751.short>
- [6] T. Mahalingam, A. Kathalingam, *Electrodeposition and characterization of HgSe thin films*, J. Materials Characterization. 58, (2007) 735-739.  
<https://www.sciencedirect.com/science/article/pii/S1044580306003494>

- [7] A. Mujica, A. Rubio, A. Munoz, R. J. Needs, *High- pressure phases of group-IV, III-V, and II-VI compounds*, Reviews of modern physics, vol. 75, (2003) 863-913.  
<https://journals.aps.org/rmp/abstract/10.1103/RevModPhys.75.863>
- [8] F.EL.Haj Hassan, B.I.Shafaay ,H.meradij , S Ghemid, H Belkhir and M .Korek, *Ab initio study of fundamental properties of HgSe ,HgTe and their HgSe<sub>x</sub>Te<sub>1-x</sub> alloys* ”Phys.Scr.84, (2011) 065601-065607.  
[https://www.researchgate.net/profile/F\\_El\\_Haj\\_Hassan/publication/258325074](https://www.researchgate.net/profile/F_El_Haj_Hassan/publication/258325074)
- [9] M. N. Secuk, M. Aycibin, B. Erdinc, S. E. Gulebaglan, E. K. Dogan,H. Akkus “*Ab initio calculation of structural, electronic, optical, dynamic and thermodynamic properties of HgTe and HgSe* “American Journal of Condensed Matter Physics , 4(1), (2014) 13-19.  
[https://www.researchgate.net/profile/Mehmet\\_Secuk/publication/265166804](https://www.researchgate.net/profile/Mehmet_Secuk/publication/265166804)
- [10] [Http://www.quantum-espresso.org](http://www.quantum-espresso.org).
- [11] S. Ahmadi and M.H. Ramezani . *The structural and density state calculation of Boron and Nitrogen doped silicene nano flake*, Journal of Optoelectrical Nanostructures Vol. 2.No1(2017)41-48.  
<http://jopn.miau.ac.ir/>
- [12] O. Madelung, M. Schulz, Numerical Data and Functional Relationships in Science and Technology, Group III, Landolt-Bornstein, Berlin, vol. 22a, (1987) 219-220.
- [13] S. H. Wei, A. Zunger, *Calculated natural band offsets of all II–VI and III–V semiconductors*, Phys. Rev. B39, (1989) 1871-1883.  
<https://aip.scitation.org/doi/abs/10.1063/1.121249>
- [14] *Handbook of Crystallographic Data for Inter metallic phases*, P. Villars, L. D. Calvert, 2nd Edition, (Asm International, Metals park, OH, 1985).
- [15] G. Arora, B. L. Ahuja, *Electronic Structure of some mercury chalcogenides using compton spectroscopy*, J. Radiation Physics and Chemistry. 77, (2008) 9-17.  
<https://www.sciencedirect.com/science/article/abs/pii/S0969806X07003015>
- [16] *Handbook on Physical Properties of Semiconductors*, S. Adachi, Kluwer Academic, New York, Boston, vol. 3, (2004) 420.
- [17] K. U. Gawlik, L. Kipp, M. Skibowski, N. Orlowski, and R. Manzke, *HgSe :Metal or semiconductor*. Phys. Rev. Lett 78, (1997) 3165-3168.  
<https://journals.aps.org/prl/abstract/10.1103/PhysRevLett.78.3165>

- [18] *Handbook of optics*, M. Bass, G. Li, E. V. Stryland, 3<sup>th</sup> Edition, The McGraw-Hill Companies, (2010).
- [19] H. Salehi, P. Amiri and R. Zare Hasanabad. *Ab-initio Study of Electronic, Optical, Dynamic and Thermoelectric Properties of  $CuSbX_2$  ( $X=S, Se$ ) Compounds*, Journal of Optoelectronic Nanostructures Vol. 3.No2(2018)53-64.  
<http://jopn.miau.ac.ir/>
- [20] *Handbook of Condensed Matter and Materials Data*, W. Martienssen, H. Warlimont, Springer, (2004).
- [21] P. L. Deboeij, F. Kootstra, J. G. Snijders, *Relativistic Effects in the Optical Response of HgSe by Time-Dependent Density Functional Theory*, J. Quantum Chemistry. 85, (2001) 449.  
<https://onlinelibrary.wiley.com/doi/abs/10.1002/qua.1516>

